Geomechanics and Engineering, *Vol. 33, No. 6 (2023) 583-596*
https://doi.org/10.12989/gae.2023.33.6.583

Impact of soft and stiff soil interlayers on the pile group dynamic response under lateral harmonic load

Masoud Oulapour*, Sam Esfandiari[a] and Mohammad M. Olapour[b]

Department of Civil Engineering, Faculty of Civil Engineering and Architecture, Shahid Chamran University of Ahvaz, Ahvaz, Iran

(*Received May 19, 2022, Revised April 17, 2023, Accepted May 4, 2023*)

Abstract. The interlayers, either softer or stiffer than the surrounding layers, are usually overlooked during field investigation due to the small thickness. They may be neglected through the analysis process for simplicity. However, they may significantly affect the dynamic behavior of the soil-foundation system. In this study, a series of 3D finite-element Direct-solution steady-state harmonic analyses were carried out using ABAQUS/CAE software to investigate the impacts of interlayers on the dynamic response of a cast in place pile group subjected to horizontal harmonic load. The experimental data of a 3×2 pile group testing was used to verify the numerical modeling. The effects of thickness, depth, and shear modulus of the interlayers on the dynamic response of the pile group are investigated. The simulations were conducted on both stiff and soft soils. It was found that the soft interlayers affect the frequency-amplitude curve of the system only in frequencies higher than 70% of the resonant frequency of the base soil. While, the effect of stiff interlayer in soft base soil started at frequency of 35% of the resonant frequency of the base soil. Also, it was observed that a shallow stiff interlayer increased the resonant amplitude by 11%, while a deep one only increased the resonant frequency by 7%. Moreover, a shallow soft interlayer increased the resonant frequency by 20% in soft base soils, whereas, it had an effect as low as 6% on resonant amplitude. Also, the results showed that deep soft interlayers increased the resonant amplitude by 17 to 20% in both soft and stiff base soils due to a reduction in lateral support of the piles. In the cases of deep thick, soft interlayers, the resonant frequency reduced significantly, i.e., 16 to 20%. It was found that the stiff interlayers were most effective on the amplitude and frequency of the pile group.

Keywords: ABAQUS/CAE; dynamic response; interlayer; pile group; resonant amplitude; resonant frequency

1. Introduction

Deep foundations are used underneath most infrastructures, such as industrial structures, bridges, towers, and wind turbines. Their response to dynamic and cyclic loading is a crucial element in the design of superstructures. The vibrations could be caused by vibratory machinery, wind, earthquake, and traffic. Several pieces of research have been conducted on the dynamic interaction of soil-pile-structure systems. (Barari *et al.* 2021, Chong *et al.* 2019, Kim and Choi 2017, Poorjafar *et al.* 2021, Shi *et al.* 2018). Horizontal vibrations are an essential aspect of the behavior of these piles. Although the dominant forms of waves in natural loading are random and periodic vibrations, the regular harmonic (sinusoidal) form is usually used to simplify the design process (Arshad and O'Kelly 2016, API RP 2A-WSD, 2014).

Some of the studies on the dynamic behavior of piles have focused on the vibrations of single piles (Bhowmik *et al.* 2013, Chiou *et al.* 2018, Gerolymos *et al.* 2009, Hong *et al.* 2017, Kahribt and Abbas 2018, Zhang and Ng 2017, Zhu *et al.* 2021). However, numerous studies in the literature deal with pile group behavior (Al-Omari *et al.* 2019, Chandrasekaran *et al.* 2010, Kaynia and Kausel 1982, Luan *et al.* 2019b). Kaynia and Kausel (1982) concluded that the dynamic behavior of a group of piles is very sensitive to frequency and presented several diagrams of dynamic soil-pile interaction coefficients. For example, in a specific frequency range, a pile group may show a stiffness more than the total stiffness of all individual piles in that group. Also, the central piles in the group may carry a significant part of the exerted loads compared to the edge piles (Kaynia and Kausel 1982).

Several analytical and numerical methods are developed to study the interaction of pile and soil that is arisen by the difference between the stiffness of pile and soil and the difference between the boundary conditions of the piles. Some of the researchers modeled soil as a continuous, viscous material having a hysteretic damping, while the pile was considered as a linear elastic beam. In the Winkler model, the soil is replaced with springs. It has been shown that even though the Winkler model leads to reasonable responses under static loadings, it is susceptible to the choice of moduli in dynamic conditions, and it is not capable of modeling frequency dependence behavior or resonance (Zheng *et al.* 2016, Anoyatis *et al.* 2016, Anoyatis and Lemnitzer 2017, Cao and Zhou 2020, Wang *et al.* 2014). In order to consider the soil shear behavior and damping, some researchers used the Pasternak model (Dobry and Gazetas 1988, Cetin and Simsek 2011, Zhou *et al.* 2006). In this model, the dynamic interaction of soil and

*Corresponding author, Associate Professor
E-mail: Oulapour_m@scu.ac.ir
[a]Graduate Student
[b]Graduate Student

ISSN: 2005-307X (Print), 2092-6219 (Online)

pile is studied using dashpots and springs at the interface and complex functions for the impedance. The real terms of these functions account for the stiffness of pile and soil, and the imaginary terms account for both material and geometric dampings. (Dobry and Gazetas 1988, Park and Hashash 2004, Yang *et al.* 2018, Zhang *et al.* 2021). Zhou and Wang (2009) analyzed the dynamic response of pile groups using the Muki and Sternberg approach as well as the superposition method. The Fredholm integral of the second kind is used to articulate the load transfer problem. Generally, axial and lateral loads are applied to the pile foundations concurrently. The axial force has a second-order effect on the horizontal displacements and frequency contents of vibrations under dynamic horizontal loading (Catal 2006, Ding *et al.* 2017, Fayyazi *et al.* 2014). The interaction of single piles and soil media is studied employing different methods. Lysmer and Kuhlemeyer (1969) suggested using energy-absorbing viscous dampers for modeling infinite domains. A method based on nonlinear p-y curves was established by Nogami *et al.* (1992) in order to consider the behavior of the soil surrounding piles in the time domain analysis of pile groups. Also, using the t-z springs method, the effect of stress reversal during cyclic loading, which leads to irrecoverable strains and subsequent degradation of stiffness of pile surrounding soil, showed that the effect of anti-overturning moment reduces noticeably (Shao *et al.* 2019, Wang *et al.* 2020). Similarly, several experimental studies were performed. Some of these studies were conducted on small-scale prototypes (Liang *et al.* 2021, Liao *et al.* 2021). Qin and Guo (2016) found that the cyclic load amplitude had a more significant impact than the number of cycles, and the dynamic subgrade modulus was 1.5–2.8 times of the static one. Despite the high expenses of field full-scale tests, quite a few studies have been reported (Choudhary *et al.* 2016, El-Marsafawi *et al.* 1992, Novak and El-Sharnouby 1984). The centrifuge experiments provided valuable findings (Sungyani and Desai 2017, Tamura *et al.* 2021, Wang *et al.* 2021, Zhang *et al.* 2008). Kong *et al.* (2021) derived an explicit model for the development of excess pore water pressure, which is caused by the accumulation of lateral pile displacement in cyclic loading and is related to the loading rate.

Several aspects of pile group dynamics under complex conditions have been studied using numerical methods. Effect of soil or pile nonlinearity on pile's dynamic behavior has been studied extensively (Ghayoomi *et al.* 2018, Huang *et al.* 2021, Singh and Patra 2021, Zhang *et al.* 2020, Zheng *et al.* 2013). Tantayopin and Thammarak (2017) conducted experiments on three floating piles and simulated the response numerically to examine the effect of a thick, soft clayey layer located over a stiff clay on the resonance of the piles. They concluded that the local resonances of the pile–soil system necessitates the consideration of the entire extent of the soft soil layer. Basack and Nimbalkar (2018) indicated that in soft soil, the cyclic-loading parameters, such as the number of cycles, frequency, and amplitude of vibrations have significant effect on the pile lateral displacements and its capacity. Also, it was observed that at low to medium frequencies, the effect of soil nonlinearity on pile response was substantial, but at higher frequencies, it was virtually ineffective. Manna and Baidy (2010) found that increasing the spacing of piles increases the damping and stiffness of the pile group. Ladhane and Sawant (2016) studied the effect of pile group configuration and proved that decreasing the spacing of piles results in an increase in peak amplitudes. In addition, if the length to diameter ratio (L/D) is increased, the mass of the vibrating system increases too, while the fundamental frequency decreases. Also, the nonlinearity of the soil behavior results in the reduction of fundamental frequencies as the stiffness reduces. Choudhary *et al.* (2016) indicated that increasing the excitation force reduces the resonant frequencies, and the frequency-amplitude curves show nonlinearity and the amplitudes are not proportional. Very few researches focused on the effect of *layering of soils* (Kaynia and Kausel 1991, Wang *et al.* 2014, Ai *et al.* 2016, Ding *et al.* 2020, Jiang and Ashlock 2020). Kaynia and Kausel (1991) used the Green function-based analytical method to analyze the behavior of single piles and pile groups in layered soils under plane-strain conditions. They indicated that, in nonhomogeneous soils, the interaction between the pile and adjacent soil is significant, imposing abrupt changes on impedance functions. These changes would be more remarkable in softer soils. Maeso *et al.* (2005) employed the Boundary Element Method to calculate impedance functions for pile groups in saturated porous media.

Wang *et al.* (2014) used the layered Pasternak foundation to consider the soil shear strains in obtaining the transfer matrix and the horizontal impedance of a single pile. It was proved that the shear strains in the soil have remarkable impact on the impedance of group of piles, especially in the case of low pile–soil modulus ratio.

The effect of *pile installation method and conditions* on the behaviour of pile group under lateral cyclic loading is rarely studied (Fattah *et al.* 2021a, Fattah *et al.* 2021b). Staubach *et al.* 2022 performed a series of numerical simulations to compare long term behaviour of group of piles installed by vibratory and impact driving methods under cyclic lateral loading. It was concluded that the installation method has a minor effect compared to the effect of drainage conditions around the pile during installation. Fattah *et al.* (2016) conducted a series of laboratory tests and concluded that for soil bed in dry state, for both loose and medium dense soils, the acceleration amplitudes increase with frequency for both soil relative densities.

Although many studies have been performed on the pile dynamic response, less attention has been paid to the effects of diversity of the properties of soil layers. Sometimes, thin interlayers composed of materials different from adjoining layers, are overlooked or not identified during field explorations. Therefore, it is necessary to elaborate the effect of such interlayers on the dynamic response of pile groups and to correlate the weak-zone properties with the vibration amplitude. Considering that Offshore Wind Turbines are supported by groups of piles, the natural frequency of such pile groups is a very important issue.

In this study, the field experiments performed by El-Marsafawi *et al.* (1992) on the pile group under horizontal

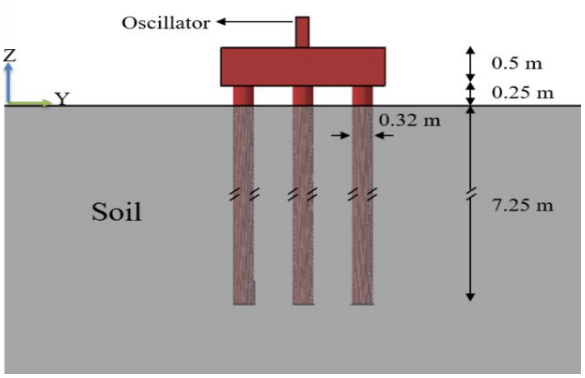

Fig. 1 Schematic diagram of the test setup

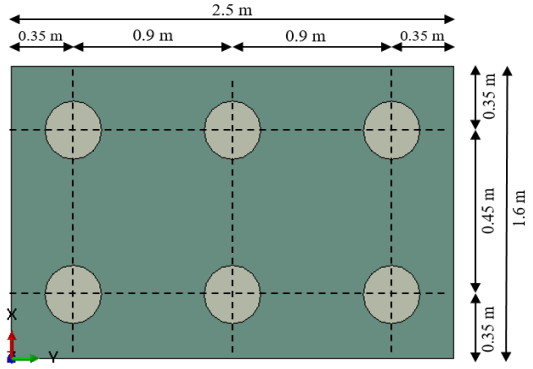

Fig. 2 Pile cap dimensions and pile spacing in the experiments

dynamic load were used to validate numerical modeling using ABAQUS finite element software. Soil-pile interaction, nonlinear soil behavior, and semi-infinite geometry of media were considered. The effects of presence of an unnoticed soft or stiff interlayer on the dynamic behaviour of a group of cast in place concrete piles under horizontal harmonic load were studied. In this regard different thicknesses, depths, and shear modulus ratios of the interlayer cast in either soft or stiff base soils were considered. The frequency-amplitude curve, resonant frequency and amplitude of vibrations at resonant frequency were studied. As this paper is based on the tests on cast in place pile groups, the results can only be extended to this method of installation.

2. Field experiments

The results of large-scale field experiments on a group of 3×2 steel piles, installed into layered soils and conducted by El-Marsafawi *et al.* (1992), were used in this research. In these experiments, horizontal dynamic loads with different intensities and frequencies were applied to the system using a mechanical oscillator placed on the top of the pile cap.

The vibrometers (LVDTs) were placed on the top of the pile cap to record the lateral displacements of the pile foundations up to a steady state. Subsequently, frequency-amplitude curves of the systems were obtained by combining the results of the experiments for any specific dynamic load intensity. The general outline of the experiments and the pile group configuration are shown in Figs. 1 and 2.

Table 1 Material properties of the piles and pile cap

γ (KN/m^3)	E(MPa)	υ
24.5	19.6	0.2

2.1 Materials and system characteristics

In the experiments, the diameter and length of piles were 0.32 m and 7.5 m, respectively. The piles were connected to a 1.6×2.5 m pile cap, and the base of the pile cap was placed 0.25 meters above the ground surface. Table 1 presents the material properties of the piles and pile cap and Table 2 presents the properties of the soil layers, which were obtained by laboratory triaxial and in-situ downhole tests.

2.2 Test procedure

The field experiments were conducted on the cast-in-situ concrete pile group to investigate the dynamic response of the system under horizontal harmonic, dynamic loads. The load was generated by a mechanical oscillator with two counter-rotating eccentric masses. This oscillator produced quadratic centrifugal force proportional to the square of the circular frequency of the excitation. The equation of the generated force is

$$F(t) = (m_e e)\omega^2 \cos(\omega t) \quad (1)$$

where m_e represents the mass of the eccentric rotating part of the oscillator, e is the eccentricity of the masses, ω is the circular frequency, t shows time, and $m_e e$ is the intensity of exciting force. Also, the normalized response amplitude for translation is defined as follows

$$A = \left(\frac{m}{m_e e}\right) u \quad (2)$$

where A is the dimensionless response amplitude, m is the vibrating mass (the pile cap and the oscillator), and u is the horizontal displacement measured on the top of the pile cap. Moreover, the oscillator was placed on top of the pile cap and fully attached to it. So, the exciting force acted 0.2 m above the pile cap surface in the X-direction. The vibrometers were placed at the top of the pile cap to measure the lateral displacements. As the test started, the rotational speed of the motor was increased gradually, generating a harmonic horizontal force according to Eq. (1), and the vibrometers measured the displacements simultaneously. The test was repeated at different frequencies, and by combining the obtained results, the frequency-amplitude diagram of the system was established. The setup of the experiment is presented in Fig. 3.

The previous experiments were conducted for different exciting intensities. In the present study, the experiment with exciting intensity of $m_e e$=0.259 kg.m was used for numerical simulations.

Table 2 Mechanical properties of the soil layers at the site (El-Marsafawi *et al.* 1992)

Z (m)	ρ (Kg/m3)	υ	Vs (m/s)	E (MPa)	C (KPa)	φ (º)
0-1	2060	0.3	130	90.5	35	25
1-2	2060	0.3	193	199.5	35	25
2-3	1890	0.3	200	196.6	25	20
3-4	1890	0.3	180	159.2	25	20
4-5	2010	0.3	234	286.2	30	25
5-6	2010	0.3	272	386.6	30	25
6-7	2010	0.3	272	386.6	30	25
7-20	2040	0.3	280	415.8	30	25

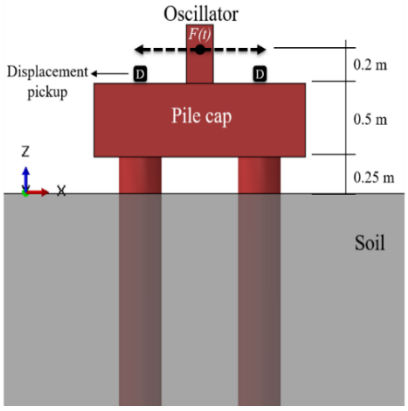

Fig. 3 The test setup experiments, El-Marsafawi *et al.* (1992)

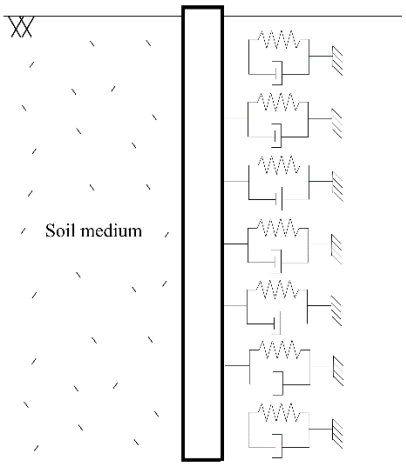

Fig. 4 Pile structure as a beam resting on Winkler foundation

3. Finite element analysis

The three-dimensional geometric models have been used to model the soil-pile group system. For this purpose, different parts of the system, including soil, pile, and pile cap models, were generated separately. Then, these models were assembled to reach the geometric model of the system, which was analyzed using ABAQUS/CAE software. The details of the finite element modeling techniques are provided in the following sections.

3.1 System governing equations

The analytical formulation of the pile-soil dynamic interaction can be approached as the classic beam on elastic foundation problem. The governing differential equation of vibrations of an Euler-Bernoulli beam on the elastic foundation can be formulated as

$$EI\frac{\partial^4 w(z,t)}{\partial z^4}+\rho A\frac{\partial^2 w(z,t)}{\partial t^2}+k(z)w(z,t)=0 \qquad 0\le z\le L \tag{3}$$

where *w(z,t)* is the displacement at a depth of z and time t, *L* is the length of the beam, *EI* is the beam bending rigidity, *ρA* is the mass per unit length, and *k(z)* is the modulus of subgrade reaction of soil at depth *z*. Fig. 4 shows the configuration of a beam with a constant cross-section.

The method of separation of variables or the Fourier method can be utilized to solve the differential equations of dynamic equilibrium. Therefore, the displacement w is expressed as

$$w(z,t)=\bar{w}(z)e^{i\omega t} \tag{4}$$

where ω is the circular natural frequency of each mode of vibration, and $\bar{w}(z)$ shows the corresponding mode shape. Substituting the new form into the governing differential equation, Eq. (3) is transformed to

$$EI\frac{\partial^4 \bar{w}}{\partial z^4}-\rho A\omega^2\bar{w}+k(z)\bar{w}=0 \tag{5}$$

The foundation is characterized by a group of springs that can be either linear elastic or nonlinear elastic, or even viscoelastic, as in the Pasternak model. The boundary conditions at the top where the piles are connected to the pile cap can be given as

$$\ddot{w}=\frac{\partial^2 w}{\partial t^2}=\frac{F(t)}{M_{piles\ and\ pile\ cap}} \quad \text{at} \quad z=0\ and\ t\ge 0 \tag{6}$$

Furthermore, the boundary conditions at the free tip of the pile are

$$\frac{\partial^2 w}{\partial z^2}=\frac{\partial^3 w}{\partial z^3}=0 \ \text{ at } z=L\ and\ t\ge 0 \tag{7}$$

These governing equations subjected to the specified initial and boundary conditions have been solved using

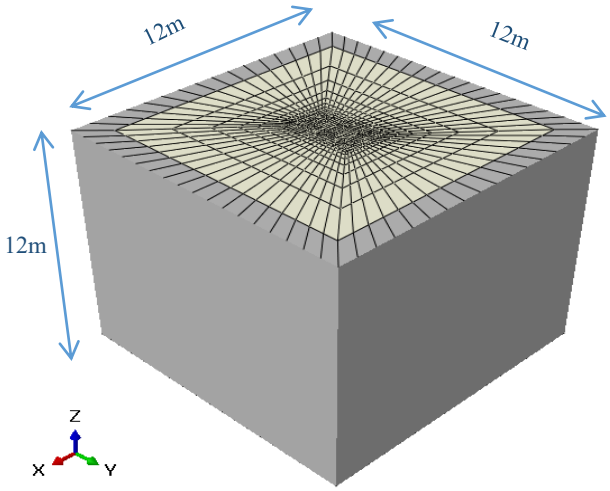

Fig. 5 Overview of the soil boundary conditions in the finite element model

several different methods (Kaynia and Kausel 1991, Wang *et al.* 2014, Ai *et al.* 2016, Ding *et al.* 2020). In this research finite element method based ABAQUS/CAE software was used.

3.2 Lateral boundary conditions

Soil is a semi-infinite media, and it is impossible to model the entire medium numerically; Therefore, only a limited part of the soil media can be modeled. Besides, dynamic loading produces various waves in soil media which spread to the far-field. However, truncating the soil media at the model boundaries and close to the source of the waves leads to reflection of the waves. This produces a disturbance in the model and makes the modeling unrealistic. On the other hand, modeling a large soil medium prolongs the analysis process. In the previous studies, various methods such as viscous transmitting boundaries and Kelvin elements have been used to manage the problem of unreal wave reflection at boundaries (Chung and Yang 2017, Ladhane and Sawant 2016, Lysmer and Kuhlemeyer 1969). One of the best methods to simulate the semi-infinite soil medium is to use energy-absorbing boundaries such as infinite elements as boundary conditions (Luan *et al.* 2019a, Wen *et al.* 2015). A sensitivity analysis was performed on the dimensions of the model by changing the location of lateral boundaries in order to minimize the reflection of waves and calculation time simultaneously. Also, the infinite elements are used at truncated boundaries to increase the accuracy of simulation of the semi-infinite soil medium. The dimensions and boundary conditions of the model are shown in Fig. 5.

3.3 System damping

The system's damping consists two parts: geometric damping and material damping. The geometric damping is due to the attenuation of the wave energy as it propagates. In this study, the geometric damping is accounted for by considering the appropriate dimensions obtained from the sensitivity analysis of the model dimensions and using infinite elements as soil boundary conditions. Furthermore, material damping, which depends on material properties, is denoted by the Rayleigh damping. The Rayleigh damping is defined as the combination of the mass and stiffness matrices of the system as

$$[C_m] = \alpha_r[M] + \beta_r[K] \tag{8}$$

If the damping ratio of the soil profile is assumed to be constant and equal to ξ between the first two significant natural modes of vibrations, then the circular frequencies of these modes of the system, ω_1 and ω_2, can be used to find the corresponding α_r and β_r (Park and Hashash 2004, ABAQUS/CAE manual 2016) as in Eqs. (9) and (10).

$$\alpha_r = \frac{2\xi\omega_1\omega_2}{\omega_1+\omega_2} \tag{9}$$

$$\beta_r = \frac{2\xi}{(\omega_1 + \omega_{2)}} \tag{10}$$

Therefore, in this study ω_1 was assumed equal to the resonant circular frequency of the system obtained from field experiments (151 rad/sec). Also, ω_2 was assumed equal to the circular frequency of the exciting harmonic force from the oscillator. Similarly, the critical damping ratio of the soil profile was assumed to be constant and equal to 0.035 (El-Marsafawi *et al.* 1992). Therefore, the Rayleigh damping coefficients of the system were calculated for each load with a different excitation frequency.

3.4 Soil-pile interaction

Applying lateral dynamic load to the soil-pile system may cause slippage and separation between the pile body and the adjacent soil along a limited extent of the pile near the ground surface. Various numerical techniques have been used to study the interaction of surfaces in contact with each other (Peric and Owen 1992). In order to consider the interaction effect between the pile and surrounding soil, Ladhane and Sawant (2016) suggested employing surface elements and using the Kelvin elements to prevent stress

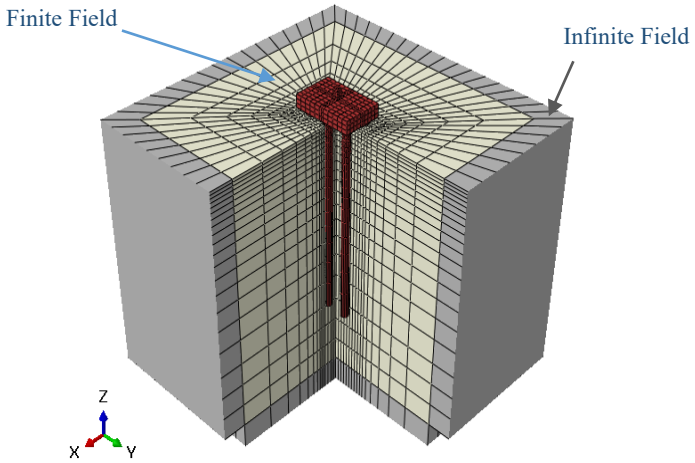

Fig. 6 The finite element mesh of the system for the field experiment

wave radiation. Also, Sarkar and Maheshwari (2012) modeled the effect of separation and slippage at soil-pile surface-to-surface contact by employing contact elements.

In this study, following Biswas and Manna (2014), the surface-to-surface contact element, a feature of ABAQUS/CAE, was used to incorporate the interaction between the piles and the soil. Moreover, the pile and soil were introduced as master and slave surfaces, respectively, as the piles are more rigid than the surrounding soil and transmit the oscillator's force to the soil. This type of contact element includes both tangential (frictional) and normal behaviors. The finite-sliding formulation was used for tangential behavior to allow modeling of any arbitrary motion of the surfaces. The normal contact between the surfaces was simulated using a hard-contact formulation to avoid the penetration of the slave surface into the master surface and the transfer of tensile stress. However, the separation of the surfaces was probable. Also, in the hard-contact formulation, the surfaces could re-contact after separation (ABAQUS/CAE manual 2016). The tie-constraint was applied at the connection of piles to their cap, which forms a fixed connection, in order to consider their integrity.

3.5 Finite element mesh and elements type

In order to produce reliable numerical results with acceptable accuracy, a suitable mesh type, meshing method, and element size must be chosen based on the behavior of each part. Hence, each system part is discretized into a symmetrically structured mesh. Moreover, a suitable fine mesh is employed in the vicinity of stress concentration regions, such as the interface of piles and their surrounding soil, and the connection between piles and pile cap, and load application points. The mesh becomes coarser as it distances from the stress concentration areas, and infinite elements are used at the truncated boundaries. To perform an efficient wave propagation dynamic analysis, the ratio of the size of the elements to the wavelength must be small enough. The ratio of wavelength to element size must be at least 5 to 10 (Semblat and Brioist 2000). The measured shear wave velocity of the soil (v_s) profile at the site varies from 130 m/s to 280 m/s. Also, the predominant frequency of the waves propagated in the medium is assumed to be equal to the exciting input frequency, varying from 1 Hz to 44 Hz. Therefore, based on Equation 11, the shortest wavelength generated in the soil medium resulted from the minimum shear wave velocity of 130 m/s and the maximum input exciting frequency of 44 Hz, is equal to 2.95 m. Since a ratio of 5 is used for the shortest wavelength to the longest element size, the maximum allowable element size must be 0.6 m, which is much greater than the size of elements used in this study, especially in the vicinity of the stress concentration areas.

$$\lambda_{min} = \frac{v_{s_{min}}}{f_{max}} \tag{11}$$

The size and number of the elements affect the accuracy, computational time, and volume of analysis outputs.

Therefore, the mesh size is adjusted so that valid results with reasonable accuracy can be achieved using fewer elements while observing the maximum allowable element size. The present study is conducted using three-dimensional models and elements. This leads to an increase in the analysis time. Therefore, reduced-integration elements are utilized to decrease the computation time. For this purpose, first-order eight-node brick elements with reduced-integration (C3D8R) are used for the piles, the pile cap, and the finite field of the soil medium. Also, first-order eight-node infinite elements (CIN3D8) are used for the infinite field of the soil media. Although C3D8R elements are readily available in ABAQUS/CAE elements library, CIN3D8 elements need to be coded in the software. Fig. 6 depicts the finite element (FEM) mesh used in the model.

3.6 Constitutive equation of material

In this study, as the magnitude of the exciting force is relatively low, the pile material (concrete) behavior was assumed to be linear elastic with properties presented in Table 1. Moreover, due to the significance of soil constitutive model, a sensitivity analysis was made in order

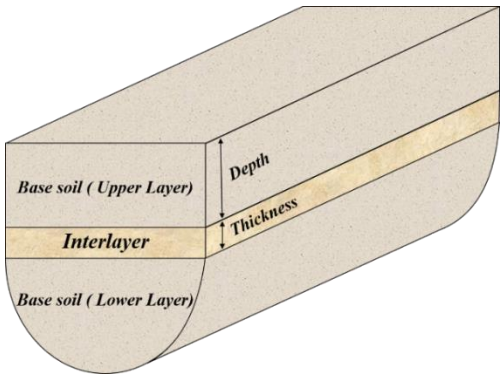

Fig. 7 Geometric configuration of an interlayer embedded in base soil

Table 3 Properties of the base soils

Properties	ρ (Kg/m^3)	ξ	υ	***Vs*** (m/s)	***E*** (MPa)	***c*** (kPa)	φ (º)
Stiff base soil	2000	0.032	0.3	220	252	35	22
Soft base soil	1600	0.036	0.3	150	94	30	20

to decide the constitutive model. Among the models included in the software, 3 models including linear elastic, Mohr-Coulomb and Drucker-Prager criteria were employed and the numerical results were compared with the experimental data. The Mohr-Coulomb plasticity model yielded the best accordance of calculation results and the experimental data. Therefore, the linear elastic Mohr-Coulomb constitutive model, presented in Eq. (12), was used to consider the soil nonlinearity.

$$\tau = \sigma_n \tan\varphi + c \tag{12}$$

The material constants of the Mohr-Coulomb criterion of each layer of the soil at the test site were selected according to Table 2.

3.7 Loading and initial conditions

The aim of the first loading step was to generate the initial soil conditions and in situ stresses of the at-rest state condition before applying any external load. For this purpose, a geostatic at rest stress state is assumed, and the gravity force was applied to the soil. The horizontal and vertical geostatic stresses increase with the depth. Subsequently, the static loads caused by the piles and the pile cap were applied to the system by utilizing a gravitational load. Next, a concentrated harmonic horizontal load with a particular frequency and intensity was applied at the location of the oscillator. The duration of application of harmonic load must be long enough to achieve a steady-state response. In this study, it was found out that a minimum duration of 3 seconds is needed to reach a steady-state response.

4. Parametric study of the effect of an interlayer in the soil profile

In this section, the details of the numerical models used for parametric analysis, such as the properties of the materials of the interlayers and the base soils and the configuration of the pile group, are presented. Fig. 7 indicates the general configuration of the soil profile, including an interlayer.

4.1 Material properties of the base soils

The experiments by El-Marsafawi *et al.* (1992) were performed in homogeneous sandy clay soil with shear wave velocity between 130 to 280 m/s. This soil is classified as a type D in ASCE/SEI 7-22 (2022) and is described as stiff soil. However, a soft base soil was used in the parametric studies in this research. Under ASCE/SEI 7-22 (2022), subsoil sections with mean shear wave velocities less than 180 m/s are classified as soft soil type E. Table 3 shows the mechanical properties of the soft and stiff base subsoils.

4.2 Configuration of the pile group

In this research, the 3×2 pile group configuration tested in the field experiments by El-Marsafawi *et al.* 1992, was used. The material properties of the piles and pile cap are assumed according to Table 1.

4.3 Configuration of the interlayers

The interlayers are characterized by their material properties and their geometry. Thickness, T, and depth, Z, are two main geometrical properties of the interlayers which significantly affect the dynamic response of the system. Also, the soil shear modulus, G, is the main property of the interlayer materials that influences the dynamic behavior of the system. The depth of the interlayers was expressed as the product of the pile diameter D and the depth ratio, Z/D. Also, the thickness of interlayer is represented by the thickness ratio, T/D. The subscript i stands for the interlayer, and subscript b indicates the base soil. Also, the

Table 4 Classification of the properties of the interlayers

Shear Modulus ratio (G_i/G_b)			Depth (Z/D)			Thickness (T/D)		
G_i/G_b	Name	Label	Z/D	Name	Label	T/D	Name	Label
1.5	G0	Stiff	3	Z1	Shallow	2	T1	Thin
0.5	G1	Medium	5	Z2	Semi-Deep	4	T2	Thick
0.125	G2	Soft	7	Z3	Deep	-	-	-
0.0625	G3	Very Soft	-	-	-	-	-	-

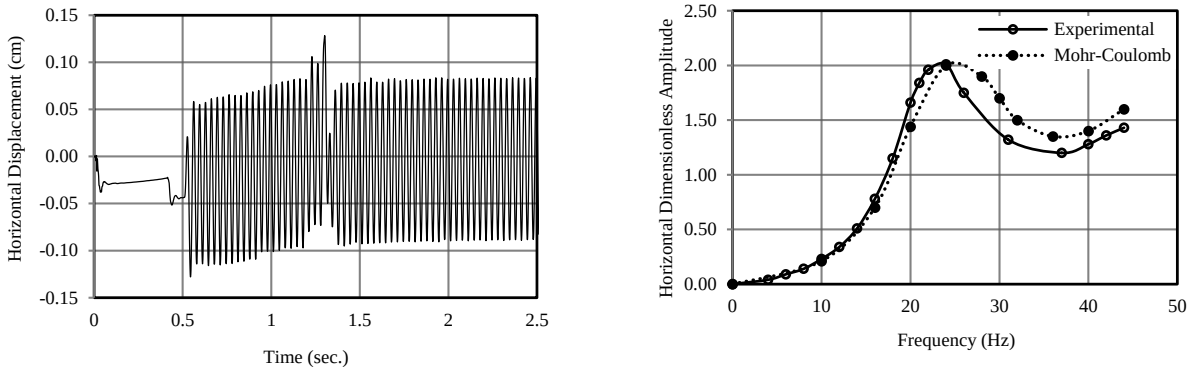

(a) Sample simulation results for a frequency of 30 Hz (b) The experimental and the numerical results

Fig. 8 The comparison of the experimental and the numerical simulation results

shear modulus of the interlayer material is introduced by the shear modulus ratio, G_i/G_b, where G_i is the interlayer shear modulus, and G_b is the base soil shear modulus. Several soil profiles can be defined through a combination of these properties. In the case of soft base soil, 24 different numerical models were analyzed. In these models, the thickness ratio (T/D) was assumed to be 2 and 4, while the depth ratio (Z/D) is equal to 3, 5, and 7. Also, the shear modulus ratio (G_i/G_b) was equal to 1.5, 0.5, 0.125 and, 0.0625. Moreover, 18 different models are analyzed in the case of the stiff base soil. These models result from the interlayer thickness ratio of 2 and 4, the depth ratio of 3, 5, and 7, and the shear modulus ratio (G_i/G_b) of 1.5, 0.5, and 0.125. Forty-two different numerical models were analyzed in two types of base soils. These interlayers with depth ratios equal to 3, 5, and 7 were named as shallow, semi-deep, and deep interlayers, respectively. Also, the thin and the thick interlayers refer to the interlayers with a thickness ratio of 2 and 4, respectively. Also, the interlayers with the shear modulus ratios (G_i/G_b) of 1.5, 0.5, 0.125, and 0.0625 were titled as stiff, medium, soft, and very soft. Table 4 presents the depth, thickness, and shear modulus ratio of the interlayers used in the numerical models. Also, the labels Homo1 and Homo2 refer to the homogeneous soft and stiff base soils without any interlayer, respectively. The symbol H1 at the end of the graph's legend refers to soft base soil, while H2 refers to stiff base soil. For instance, the numerical model presented by Z1-T2-G3-H1 indicates the case of shallow (Z/D=3), thin (T/D=2), and very soft interlayer (G_i/G_b=0.0625) located in a soft base soil (H1).

5. Numerical modeling results

5.1 Validation simulations

There is always a concern about computational simulations. In this section, the results of numerical simulations of the models developed in the previous sections, are compared with the field experiments reported by El-Marsafawi *et al.* (1992) for the exciting intensity of $m_e.e$=0.259 kg.m. Fig. 8 presents the experimental and numerical results of horizontal displacements amplitude in terms of excitation frequency. A sample of simulation of the test at a frequency of loading equal to 30 Hz is presented in Fig. 8(a). Fig. 8(b) is a composition of the results of similar simulations for different frequencies. As it is illustrated in Fig. 8(b), the experimental and the numerical results are comparable and have a similar trend. Also, there is a slight difference between the numerical and the experimental results at lower frequencies, but it increases at higher excitation frequencies. There is a 3% discrepancy in the horizontal displacement amplitude between the field experiments and the numerical results. Also, the difference between the resonant frequency of the experimental and numerical results is about 8% (2 Hz). These results indicate the validity of the numerical modeling process.

5.2 Parametric analysis

In this section, a parametric numerical analysis considering the presence of interlayers in soft and stiff base soils is presented. The effects of different properties of the interlayers, such as thickness, depth, and shear modulus

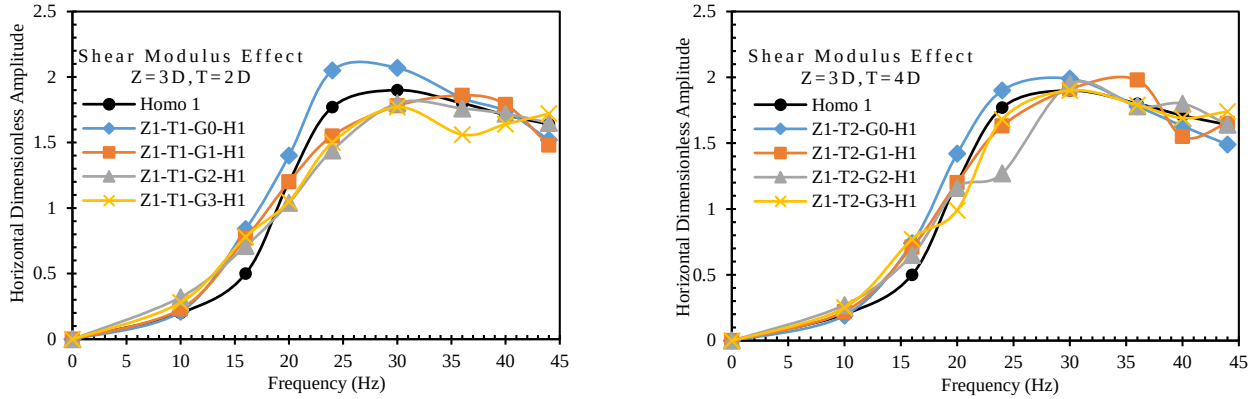

(a) Thin interlayer (T/D=2) (b) Thick interlayer (T/D=4)

Fig. 9 Frequency-amplitude response of the system with a shallow interlayer in the soft base soil (Z= 3D)

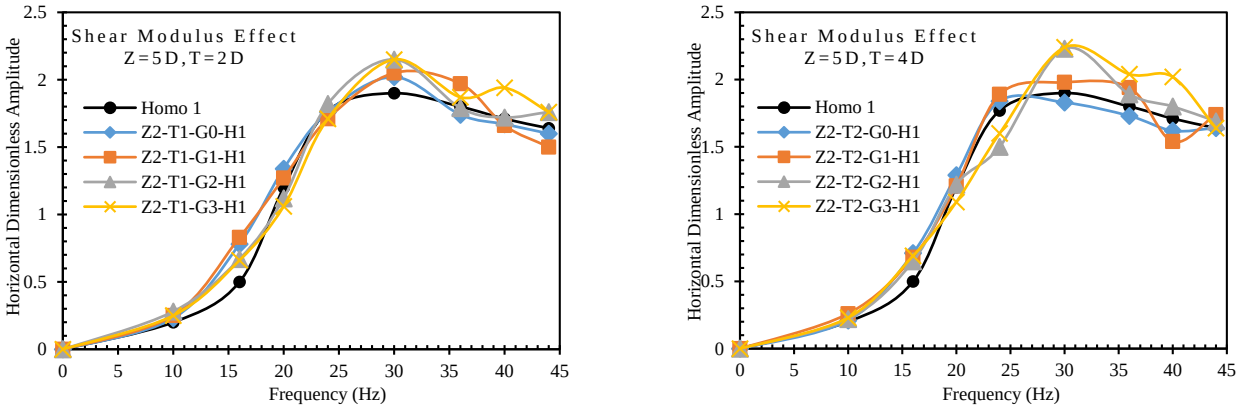

(a) Thin interlayer (T/D=2) (b) Thick interlayer (T/D=4)

Fig. 10 Frequency-amplitude response of the system with a semi-deep interlayer in the soft base soil(Z= 5D)

ratio, on the amplitude of horizontal displacements under harmonic excitations of various frequencies, are discussed.

5.2.1 Effects of interlayers in the soft base soil

Figs. 9 to12 present the results of the presence of interlayers with different thicknesses, depths, and shear modulus ratios in the soft base soil. These diagrams indicate that the interlayers have significant effect on the dynamic response of the system. This effect was more noticeable at the frequencies higher or close to the system resonance frequency. In the following sections, the effects of various parameters of interlayers on the frequency-amplitude response of the system, including the resonance frequency and amplitude, are investigated separately.

5.2.1.1 Effects of interlayers in the soft base soil on the displacement amplitude

As shown in Fig. 9(a), the presence of a shallow stiff interlayer with G_i/G_b = 1.5 increased the displacement amplitude by up to 11% at frequencies close to the resonance frequency. This was caused by the reflection of the propagating waves and trapping of the waves' energy in the space above the interlayer. Moreover, as the shear modulus ratio was reduced and the interlayer was assumed to be softer, the system response increased in excitation frequencies lower than the resonance frequency. Furthermore, due to the rise in the energy absorption and damping, there was a slight reduction of 7% in the resonance amplitude compared to the homogeneous system. However, in the case of a shallow thick interlayer, as shown in Fig. 9(b), the resonance amplitude increased slightly due to the considerable reduction in system stiffness. Also, in both shallow and deep interlayers, further reduction in the shear modulus ratio resulted an increase in the energy absorption, and subsequently, the resonance amplitude converged to the case of a homogeneous system.

As presented in Figs. 10 and 11, the presence of semi-deep and deep stiff interlayers had a slight effect on the resonance amplitude. The stiff interlayers played as an extra lateral support for the piles and reduced the vibrating length of the pile based on the stiffness of the interlayer. A ratio of 1.5 was not high enough to affect the resonance amplitude (Fig. 10).

Nevertheless, as the shear modulus ratio was reduced to 0.125, the stiffness of the interlayer soil was reduced, and the resonance amplitude increased by up to 21%, compared with the homogeneous case (Fig. 11). However, further reduction of the shear modulus ratio resulted a marginal further increase of the resonant amplitude as the shear modulus had been extremely decreased.

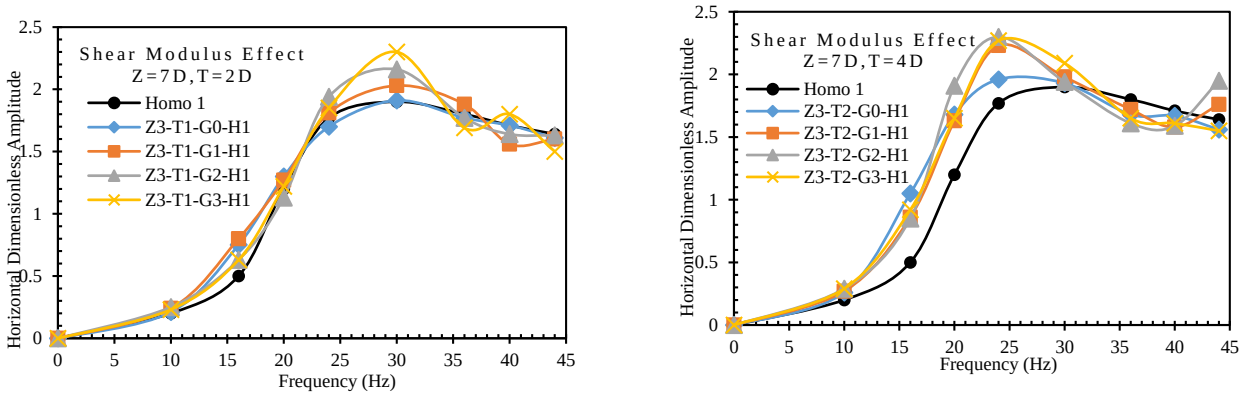

(a) Thin interlayer (T/D=2) (b) Thick interlayer (T/D=4)

Fig. 11 Frequency-amplitude response of the system with a deep interlayer in the soft base soil (Z= 7D)

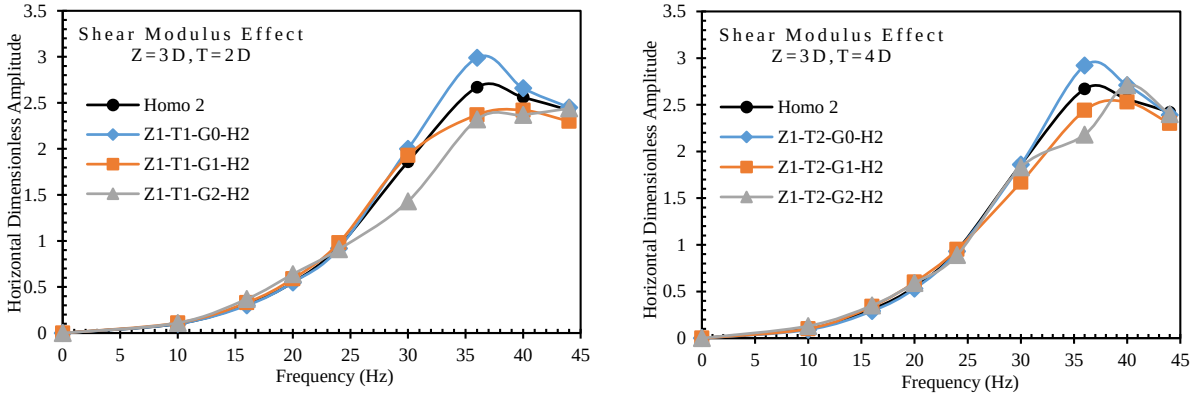

(a) Thin interlayer (T/D=2) (b) Thick interlayer (T/D=4)

Fig. 12 Frequency-amplitude response of the system with a shallow interlayer in the stiff base soil

5.2.1.2 Effects of interlayers in the soft base soil on the resonant frequency

Fig. 9 demonstrates that a shallow stiff interlayer reduced the resonance frequency by up to 13% (from 30 to 26 Hz). However, the resonance frequency increased by 23% (from 30 to 37 Hz) compared to the homogenous case, as the shear modulus ratio decreased to G_i/G_b =0.5. This is due to the development of a flexible region in the soil profile, which reduced the vibrating mass while the stiffness remained unaffected. Nevertheless, the stiffness and mass matrices decreased simultaneously as the shear modulus ratio was reduced. Thus, the resonance frequency leaned to the resonance frequency of a homogeneous system.

In the semi-deep case, a thick stiff interlayer reduced the resonance frequency up to 17% (30 to 25 Hz). The reduction was higher than the case of thin interlayer due to more reduction in vibrating length, as shown in Fig. 9. However, the reduction of the shear modulus ratio to G_i/G_b = 0.0625 caused a negligible increase in the resonant frequency, as illustrated in Fig. 10. Also, variations of the shear modulus ratio of a semi-deep thin interlayer had marginal effect on the resonance frequency due to the distance from the vibration source and its small thickness.

Fig. 11 indicates that a thick stiff interlayer reduces the resonant frequency by 13% (30 to 26 Hz) due to reduction in the vibrating length of piles. This increases the stiffness and reduces the mass of the vibrating part of the pile, which increases the natural frequency of piles. Also, as the shear modulus ratio declines to G_i/G_b = 0.5, the stiffness decreases, and subsequently, the resonant frequency decreases by 20% (30 to 24 Hz) compared to the homogeneous system. However, further reduction in the shear modulus ratio makes no difference in resonant frequency. In the higher depths, as presented in Fig. 11, a thin interlayer, regardless of its stiffness, could not affect the resonance frequency because of its distance from the effective length of the piles and the low thickness.

5.2.2 Effects of interlayers in the stiff base soil

The effects of soft or stiff interlayers with various thicknesses, placement depths, and shear modulus ratios in the stiff base soil are shown in Figs. 12 to 15. These diagrams show that in the case of stiff base soil, interlayers influence the system dynamic response significantly at higher frequencies and around the resonant frequency. The influence of interlayers on the frequency-amplitude response of the system and its resonant frequency are discussed in the following sections.

5.2.2.1 Effects of interlayers in the stiff base soil on the displacement amplitude

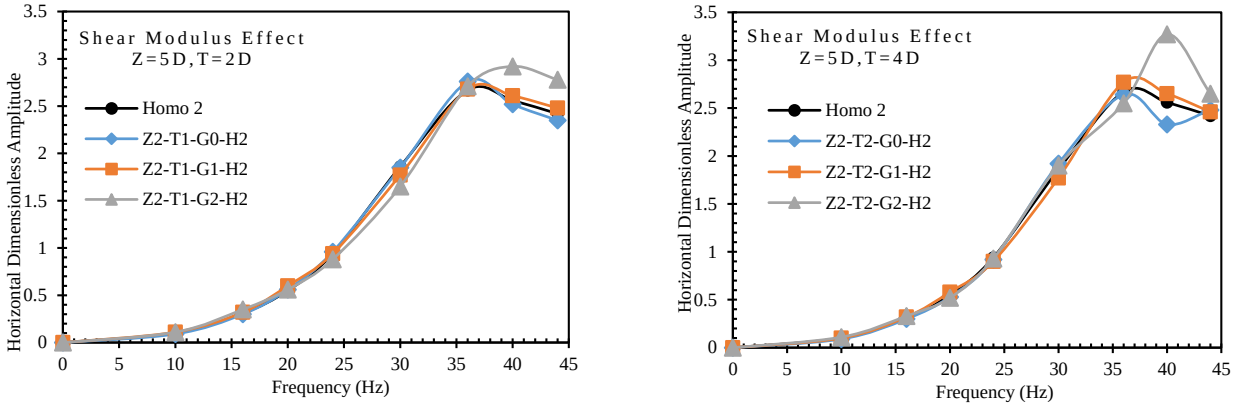

(a) Thin interlayer (T/D=2) (b) Thick interlayer (T/D=4)

Fig. 13 Frequency-amplitude response of the system with a semi-deep interlayer in the stiff base soil

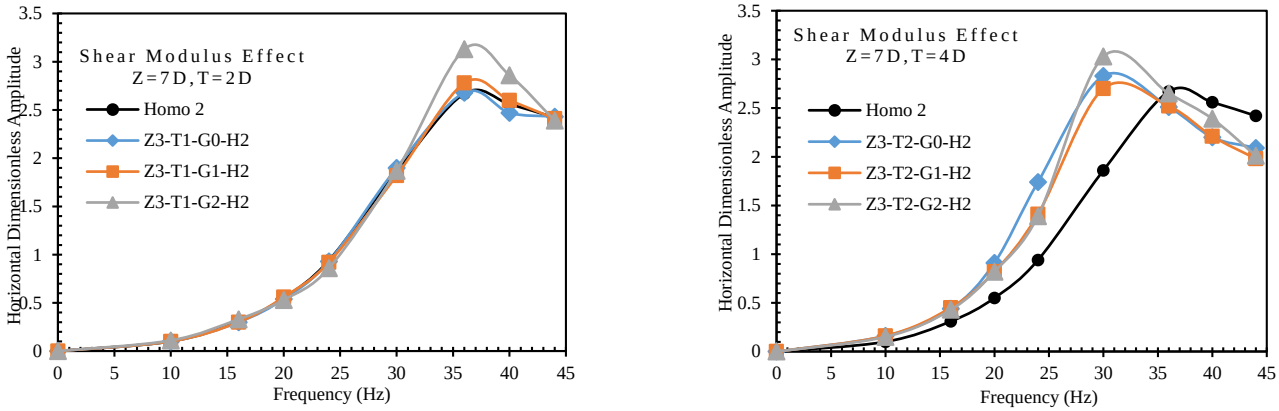

(a) Thin interlayer (T/D=2) (b) Thick interlayer (T/D=4)

Fig. 14 Frequency-amplitude response of the system with a deep interlayer in the stiff base soil

According to Fig. 12, a shallow stiff interlayer with a shear modulus of 1.5 times the surrounding soil increased the system response at the resonance or higher frequencies. It increased the system resonance amplitude by a maximum of 11% compared to the homogeneous case. This was due to the trapping of the energy of waves in the soil region above the interlayer, as the reflected waves strik the stiff interlayers. As the shear modulus ratio of the interlayer reduced to G_i/G_b = 0.5, the system response decreased in the frequency range close to the resonance frequency. And a maximum reduction of 10% occured in resonance amplitude compared to the homogenous case. This is caused by increasing the damping and energy absorption of the soft interlayer. Also, in the case of a thin interlayer, as shown in Fig. 12(a), due to the low thickness, the shear modulus reduction to G_i/G_b = 0.125 had a slight effect on the resonant amplitude in comparison with the previous cases. However, for the same shear modulus ratio of 0.125, if the interlayer is thick, as shown in Fig. 12(b), the resonant amplitude increases due to high reduction in the stiffness of lateral support of soil.

Considering Fig. 13 for the semi-deep case and Fig. 14 for the deep case, it was realized that in stiff base soils, semi-stiff or stiff interlayers have negligible effect on the frequency-amplitude response of the system since the stiffness ratio is not effective enough to affect the response, particularly if the interlayer is thin. However, in the case of a deep thick interlayer, as presented in Fig. 14, the resonance amplitude increased in the frequency range close to the resonance frequency. This increase has an inverse relation with the stiffness of the interlayer. For the case of a shear modulus ratio of 0.125, the amplitude increased by 21%. But in the case of a shear modulus ratio of 0.5 this increase was only about 4%.

5.2.2.2 Effects of interlayers in the stiff base soil on the resonant frequency

Figs. 12 and 13 illustrate that shallow and semi-deep stiff (G_i/G_b >1) interlayers do not affect th e resonance frequency. Nevertheless, as the shear modulus ratio of the interlayer was reduced to G_i/G_b = 0.125 and it was assumed to be softer, its presence effect increased the resonance frequency up to a maximum of 8% compared to the homogenous case. This was because of the consequent reduction in the vibrating mass matrix. Also, a thin deep interlayer, regardless of its stiffness, did not affect the resonance frequency of the system, Fig. 14(a). However, a thick deep stiff interlayer reduced the resonance frequency by up to 16% compared to the homogenous case, as shown in Fig. 14(b). Also, by decreasing the shear modulus ratio to G_i/G_b = 0.5, owing to a reduction in the stiffness, the

resonant frequency declined by 16% (37 to 31 Hz) in comparison to the homogeneous state. Although, a further reduction of the shear modulus ratio to $G_i/G_b = 0.125$ does not change this value.

6. Conclusions

The experimental data of a pile group were used for verification of numerical model and a parametric study was carried out to investigate the impact of interlayer properties on the dynamic behaviour of the system using three-dimensional finite element software ABAQUS/CAE. The results lead to a better understanding of the dynamic behavior of cast in place pile groups. The results are limited to the range of experimental data collected during the field tests. Also, the prescribed constitutive models in the software confine the accuracy of results. The major conclusions of this research on the impact of interlayer on the behaviour of cast in place pile are as follows:

- The soft interlayers affect the dynamic response of the system at the range of frequencies greater than 70% of the resonance frequency of both soft or stiff base soils. However, the stiff interlayers affect the response at the resonance frequency of stiff base soils. But in soft base soils this effect started at the range of frequencies higher than 35% of resonance frequency. This revealed that stiff interlayers in soft base soils may be troublesome for vibrating machinery.
- A shallow stiff interlayer increased the resonance amplitude by 11% in soft or stiff base soils without affecting the resonance frequency. However, a deep stiff interlayer increased the resonance frequency by 7% due to reducing the vibrating length while the stiffness remained constant.
- A shallow soft interlayer increased the resonance frequency by 20% in soft base soils. But, increased the resonant amplitude in thick form by 6%. A thin deep soft interlayer does not affect the resonant frequency. However, in stiff base soils, a shallow soft interlayer reduced the resonance amplitude by 10%, while it had a marginal effect on the resonance frequency.
- A deep soft interlayer increased the resonance amplitude by 17 to 21% in both soft or stiff base soils, as it reduced the lateral support of the pile, allowing more displacements, while in the thick form, it decreased the resonance frequency significantly, 16 to 20%.
- Interlayers may significantly affect the resonance frequency and amplitude of pile groups. Hence, it is very important to investigate the presence and their properties of probable interlayers during site explorations for deep foundations.

Acknowledgements

The authors also highly appreciate the anonymous reviewers' valuable comments and constructive suggestions, which improved this paper greatly.

References

ABAQUS/CAE (2016), Analysis user's guide manual, Simulia: Providence, RI, USA.

Ai, Z., Li, Z. and Wang, L. (2016), "Dynamic response of a laterally loaded fixed-head pile group in a transversely isotropic multilayered half-space", *J. Sound Vib.*, **385**, 171-183. https://doi.org/10.1016/j.jsv.2016.09.016.

Al-Omari, R.R., Fattah, M.Y. and Kallawi, A.M. (2019), "Laboratory study on load carrying capacity of pile group in unsaturated clay", *Arab J. Sci. Eng.*, **44**, 4613-4627. https://doi.org/10.1007/s13369-018-3483-9.

Anoyatis, G. and Lemnitzer, A. (2017), "Dynamic pile impedances for laterally-loaded piles using improved Tajimi and Winkler formulations", *Soil Dyn. Earthq. Eng.*, **92**, 279-297. https://doi.org/10.1016/j.soildyn.2016.09.020.

Anoyatis, G., Mylonakis, G. and Lemnitzer, A. (2016), "Soil resistance to lateral harmonic pile motion", *Soil Dyn. Earthq. Eng.*, **87**, 164-179. https://doi.org/10.1016/j.soildyn.2016.05.004.

API RP 2A-WSD (2014), Recommended practice for planning, designing and constructing fixed offshore platforms—Working stress design. American Petroleum Institute; 200 Massachusetts Avenue, Northwest Suite 1100, Washington, DC 20001 USA.

Arshad, M. and O'Kelly, B.C. (2016), "Analysis and design of monopole foundations for offshore wind-turbine structures", *Mar. Georesour. Geotec.*, **34**(6), 503-525. https://doi.org/10.1080/1064119X.2015.1033070.

ASCE/SEI 7-22 (2022), Minimum Design Loads and Associated Criteria for Buildings and Other Structures, American Society of Civil Engineers (ASCE); Reston, Virginia, United States.

Barari, A., Zeng, X., Rezania, M. and Ibsen, L.B. (2021), "Three-dimensional modeling of monopiles in sand subjected to lateral loading under static and cyclic conditions", *Geomech. Eng.*, **26**(2),175-190. https://doi.org/10.12989/gae.2021.26.2.175.

Basack, S. and Nimbalkar, S. (2018), "Measured and predicted response of pile groups in soft clay subjected to cyclic lateral loading", *Int. J. Geomech.*, **18**(7), https://doi.org/10.1061/(ASCE)GM.1943-5622.0001188.

Bhowmik, D., Baidya, D.K. and Dasgupta, S.P. (2013), "A numerical and experimental study of hollow steel pile in layered soil subjected to lateral dynamic loading", *Soil Dyn. Earthq. Eng.*, **53**, 119-129. https://doi.org/10.1016/j.soildyn.2013.06.011.

Biswas, S. and Manna, B. (2014), "Nonlinear response of full-scale pile under machine-induced coupled vibrations", *Geo-Congress 2014 Technical Papers: Geo-Characterization and Modeling for Sustainability,* Atlanta, US, February.

Cao, M. and Zhou, A. (2020), "Fictitious pile method for fixed-head pile groups subjected to horizontal loading", *Soils Found.*, **60**(1), 63-76. https://doi.org/10.1016/j.sandf.2020.01.005.

Catal, H.H. (2006), "Free vibration of semi-rigid connected and partially embedded piles with the effects of the bending moment, axial and shear force engineering structures", *Eng. Struct.*, **28**(14), 1911-1918. https://doi.org/10.1016/j.engstruct.2006.03.018.

Cetin, D. and Simsek, M. (2011), "Free vibration of an axially functionally graded pile with pinned ends embedded in Winkler–Pasternak elastic medium", *Struct. Eng. Mech.*, **40**(4), 583-594. https://doi.org/10.12989/sem.2011.40.4.583.

Chandrasekaran, S.S., Boominathan, A. and Dodagoudar, G.R. (2010), "Experimental Investigations on the behaviour of Pile groups in clay under lateral cyclic loading", *Geotech. Geol. Eng.*, **28**(5), 603-617. https://doi.org/10.1007/s10706-010-9318-4.

Chiou, J.S., Xu, Z.W., Tsai, C.C. and Hwang, J.H. (2018), "Lateral cyclic response of an aluminum model pile in sand", *Mar. Georesour. Geotec.*, **36**(5), 554-563.

https://doi.org/10.1080/1064119X.2017.1351504.
Chong, S.H., Shin, H.S. and Cho, G.C. (2019), "Numerical analysis of offshore monopile during repetitive lateral loading", *Geomech. Eng.*, **19**(1), 79-91. https://doi.org/10.12989/gae.2019.19.1.079.
Choudhary, S.S., Biswas, S. and Manna, B. (2016), "Dynamic coupled response of 6-pile groups with different pile arrangements", *Japanese Geotech. Society Special Publication*, **2**(38), 1389-1392. https://doi.org/10.3208/jgssp.IND-15.
Chung, S.H. and Yang, S.R. (2017), "Numerical analysis of small-scale model pile in unsaturated clayey soil", *Int J Civ Eng*, **15**(6), 877-886. https://doi.org/10.1007/s40999-016-0065-7.
Ding, Z., Song, C., Chen, L. and Shi, K. (2020), "Dynamic analysis of laterally loaded single piles in sandy soils considering sliding and debonding on the pile-soil interface", *Ocean Eng.*, **217**, 107720. https://doi.org/10.1016/j.oceaneng.2020.107720.
Ding, X., Luan, L., Zheng, C. and Zhu, W. (2017), "Influence of the second-order effect of axial load on lateral dynamic response of a pipe pile in saturated soil layer", *Soil Dyn. Earthq. Eng.*, **103**, 86-94. https://doi.org/10.1016/j.soildyn.2017.09.007.
Dobry, R. and Gazetas, G. (1988), "Simple method for dynamic stiffness and damping of floating pile groups", *Geotechnique*, **38**(4), 557-574. https://doi.org/10.1680/geot.1988.38.4.557.
El-Marsafawi, H., Han, Y. and Novak, M. (1992), "Dynamic experiments on two pile groups", *J. Geotech. Eng.*, **118**(4), 576-592. https://doi.org/10.1061/(ASCE)0733-9410(1992)118:4(576).
Fattah, M.Y., Karim, H.H. and Al-Recaby, M.K.M. (2021a), "Investigation of the end bearing in pile group model in dry soil under horizontal excitation", *Acta Geotechnica Slovenica*, **1**, 79-106. https://doi.org/10.18690/actageotechslov.18.1.79-106.2021.
Fattah M.Y., Karim H.H. and Al-Recaby M.K.M. (2021b), "Vertical and horizontal displacement of model piles in dry soil with horizontal excitation", *Proceedings of the Institution of Civil Engineers – Structures and Buildings*, **174**(4), 239-258. https://doi.org/10.1680/jstbu.18.00207.
Fattah, M.Y., Karim, H.H. and Al-Recaby, M.K.M., (2016), "Dynamic Behavior of Pile Group Model in Two – Layer Sandy Soil Subjected to Lateral Earthquake Excitation", *Global J. Eng. Sci. Res. Management*, **3**(8), 57-80.
Fayyazi, M.S., Taiebat, M. and Finn, W.D.L. (2014), "Group reduction factors for analysis of laterally loaded pile groups", *Can. Geotech*., *J*., **51**(7), 758-769. https://doi.org/10.1139/cgj-2013-0202.
Gerolymos, N., Escoffier, S., Gazetas, G. and Garnier, J. (2009), "Numerical modeling of centrifuge cyclic lateral pile load experiments", *Earthq. Eng. Eng. Vib.*, **8**(1), 61-76. https://doi.org/10.1007/s11803-009-9005-8
Ghayoomi, M., Ghadirianniari, S., Khosravi, A. and Mirshekari, M. (2018), "Seismic behavior of pile-supported systems in unsaturated sand", *Soil Dyn. Earthq. Eng.*, **112**, 162-173. https://doi.org/10.1016/j.soildyn.2018.05.014.
Hong, Y., He, B., Wang, L.Z., Wang, Z., Ng, C. W.W. and Mašín, D. (2017), "Cyclic lateral response and failure mechanisms of semi-rigid pile in soft clay: Centrifuge tests and numerical modelling" *Can. Geotech. J.*, **54**(6), 806-824. https://doi.org/10.1139/cgj-2016-0356.
Huang, M., Liu, L., Shi, Z. and Li, S. (2021), "Modeling of laterally cyclic loaded monopile foundation by anisotropic undrained clay model", *Ocean Eng.*, **228**, Art.108915. https://doi.org/10.1016/j.oceaneng.2021.108915.
Jiang, Z. and Ashlock, J.C. (2020), "Computational simulation of three-dimensional dynamic soil-pile group interaction in layered soils using disturbed-zone model", *Soil Dyn. Earthq. Eng.*, **130**, 105928. https://doi.org/10.1016/j.soildyn.2019.105928.
Kahribt, M.A. and Abbas, J.M. (2018), "Lateral response of a single pile under combined axial and lateral cyclic loading in sandy soil", *Civil Eng. J.*, **4**(9), 1996-2010. https://doi.org/10.28991/cej-03091133.
Kaynia, A.M. and Kausel, F. (1982), "Dynamic behavior of pile groups", *Proceedings of the 2nd International Conference on Numerical Methods in Offshore Piling*, 1982. Austin, Texas.
Kaynia, A.M. and Kausel, E. (1991), "Dynamics of piles and pile groups in layered soil media", *Soil Dyn. Earthq. Eng.*, **10**(8), 386-401. https://doi.org/10.1016/0267-7261(91)90053-3.
Kim, Y.S. and Choi, J.I. (2017), "Nonlinear numerical analyses of a pile-soil system under sinusoidal bedrock loadings verifying centrifuge model test results", *Geomech. Eng.*, **12**(2), 239-255. https://doi.org/10.12989/gae.2017.12.2.239.
Kong, D., Zhu, J., Long, Y., Zhu, B., Yang, Q., Gao, Y. and Chen, Y. (2021), "Centrifuge modelling on monotonic and cyclic lateral behaviour of monopiles in kaolin clay", *Géotechnique*, **72**(3),1-14. https://doi.org/10.1680/jgeot.19.P.402
Ladhane, K.B. and Sawant, V.A. (2016), "Effect of pile group configurations on nonlinear dynamic response", *Int. J. Geomech.*, **16**(1). https://doi.org/10.1061/(ASCE)GM.1943-5622.0000476.
Liang, R., Yuan, Y., Fu, D. and Liu, R. (2021), "Cyclic response of monopile-supported offshore wind turbines under wind and wave loading in sand", *Mar. Georesour. Geotec.*, **39**(10), 1230-1243. https://doi.org/10.1080/1064119X.2020.1821848.
Liao, W., Wu, J., Wang, Z., Yan K. and Ouyang, F. (2021), "Experimental investigation of monopile in overconsolidated marine clay subjected to multiple cyclic lateral loading events", *Mar. Georesour. Geotec.*, **40**(8), 953-966. https://doi.org/10.1080/1064119X.2021.1958034.
Luan, L., Ding, X., Zheng, C., Kouretzis, G. and Wu, Q. (2019b), "Dynamic response of pile groups subjected to horizontal loads", *Can Geotech J.*, **57**(4), 469-481. https://doi.org/10.1139/cgj-2019-0031.
Luan, L., Zheng, C. and Kouretzis, G.P. (2019a), "Simplified three-dimensional analysis of horizontally vibrating floating and fixed-end pile groups", *Int J Numer Anal Method. GeoMech.*, **43**(16), 2585-2596. https://doi.org/10.1002/nag.2997.
Lysmer, J. and Kuhlemeyer, R.L. (1969), "Finite dynamic model for infinite media", *J. Eng. Mech. Division*, **95**(4), 859-878. https://doi.org/10.1061/JMCEA3.0001144.
Manna, B. and Baidya, D. (2010), "Nonlinear dynamic response of piles under horizontal excitation", *J. Geotech. Geoenviron. Eng.*, **136**(12), 1600-1609. https://doi.org/10.1061/(ASCE)GT.1943-5606.0000388.14.
Maeso, O., Aznárez, J.J. and García, F. (2005), "Dynamic impedances of piles and groups of piles in saturated soils", *Comput. Struct.*, **83**(10-11), 769-782. https://doi.org/10.1016/j.compstruc.2004.10.015.
Nogami, T., Otani, J., Konagai, K. and Chen, H.L. (1992), "Nonlinear soil-pile interaction model for dynamic lateral motion", *J. Geotech. Eng.*, **118**(1), 89-106. https://doi.org/10.1061/(ASCE)0733-9410(1992)118:1(89).
Novak, M. and El-Sharnouby, B. (1984), "Evaluation of dynamic experiments on pile group", *J. Geotech. Eng.*, **110**(6), 738-756. https://doi.org/10.1061/(ASCE)0733-9410(1984)110:6(738).
Park, D. and Hashash, Y.M.A. (2004), "Soil damping formulation in nonlinear time domain site response analysis", *J. Earthq. Eng.*, **8**(2), 249-274. https://doi.org/10.1080/13632460409350489.
Perić, D. and Owen, D. (1992), "Computational model for 3-D contact problems with friction based on the penalty method", *Int. J. Numer. Method. Eng*., **35**(6), 1289-1309. https://doi.org/10.1002/nme.1620350609.
Poorjafar, A., Esmaeili-Falak, M. and Katebi, H., (2021), "Pile-soil interaction determined by laterally loaded fixed head pile group", *Geomech. Eng*., **26**(1), 13-15.

https//doi.org/10.12989/gae.2021.26.1.013.
Qin, H. and Guo, W.D. (2016), "Response of Static and Cyclic Laterally Loaded Rigid Piles in Sand", *Mar. Georesour. Geotec.*, **34**(2),1 38-153. https://doi.org/10.1080/1064119X.2014.979961.
Sarkar, R. and Maheshwari, B.K. (2012), "Effects of separation on the behavior of soil-pile interaction in liquefiable soils", *Int. J. Geomech*., **12**(1), https://doi.org/10.1061/(ASCE)GM.1943-5622.0000074.
Semblat, J.F. and Brioist, J. J. (2000), "Efficiency of higher order finite element for the analysis of seismic wave propagation", *J. Sound Vib*., **231**(2), 460-467. https://doi.org/10.1006/jsvi.1999.2636.
Shao, W., Yang, D., Shi, D. and Liu, Y. (2019), "Degradation of lateral bearing capacity of piles in soft clay subjected to cyclic lateral loading", *Mar. Georesour. Geotec.*, **37**(8), 999-1006. https://doi.org/10.1080/1064119X.2018.1521486.
Shi, J., Zhang, Y., Chen, L. and Fu, Z., (2018), "Response of a laterally loaded pile group due to cyclic loading in clay", *Geomech. Eng.*, **16**(5), 463-469. https://doi.org/10.12989/gae.2018.16.5.463.
Singh, S. and Patra, N.R. (2021), "Lateral dynamic response of tapered pile embedded in a cross-anisotropic medium", *J. Earthq. Eng.*, **26**, 1-22. https://doi.org/10.1080/13632469.2021.1891157.
Staubach, P., Machaček, J., Bienen, B. and Wichtmann, T., (2022), "Long-term response of piles to cyclic lateral loading following vibratory and impact driving in water-saturated sand", *J. Geotech. Geoenviron. Eng*., **148**(11). https://doi.org/10.1061/(ASCE)GT.1943-5606.0002906.
Sungyani, T. and Desai, A.K. (2017), "Seismic analysis of turbo machinery foundation: Shaking table test and computational modeling", *Earthq. Struct.*, **12**(6), 629-641. https://doi.org/10.12989/eas.2017.12.6.629.
Tamura, S., Ohno, Y., Shibata, K., Funahara, H., Nagao, T. and Kawamata, Y. (2021), "E-Defense shaking test and pushover analyses for lateral pile behavior in a group considering soil deformation in vicinity of piles", *Soil Dyn. Earthq. Eng.*, **142**, 106529. https://doi.org/10.1016/j.soildyn.2020.106529.
Tantayopin, K. and Thammarak, P. (2017), "Effect of soft soil layer on local dynamic response of floating pile under harmonic lateral loading", *Can. Geotech. J.*, **54**(12), 1637-1646. https://doi.org/10.1139/cgj-2016-0371.
Wang, J., Zhou, D. and Liu, W. (2014), "Horizontal impedance of pile groups considering shear behavior of multilayered soils", *Soils Found*., **54**(5), 927-937. https://doi.org/10.1016/j.sandf.2014.09.001
Wang, L., Zhou, W., Guo, Z. and Rui, S. (2020), "Frequency change and accumulated inclination of offshore wind turbine jacket structure with piles in sand under cyclic loadings", *Ocean Eng.*, **217**, 108045. https://doi.org/10.1016/j.oceaneng.2020.108045.
Wang, H., Wang, L., Hong, Y., Mašín, D., Li, W., He, B. and Pan, H. (2021), "Centrifuge testing on monotonic and cyclic lateral behavior of large-diameter slender piles in sand", *Ocean Eng.*, **226**, 108299. https://doi.org/10.1016/j.oceaneng.2020.108299.
Wen, X., Zhou, F., Fukuwa, N. and Zhu, H. (2015), "A simplified method for impedance and foundation input motion of a foundation supported by pile groups and its application", *Comput. Geotech*., **69**, 301-319. https://doi.org/10.1016/j.compgeo.2015.06.004.
Zhang, Y., Chen, X., Zhang, X., Ding, M., Wang, Y. and Liu, Z., (2020), "Nonlinear response of the pile group foundation for lateral loads using pushover analysis", *Earthq. Struct*., **19**(4), 273-286. https://doi.org/10.12989/eas.2020.19.4.273.
Zhang, Y. and Ng, C.W.W., (2017), "Centrifuge modeling of single pile response due to lateral cyclic loading in kaolin clay", *Mar. Georesour. Geotec.*, **35**(7), 999-1007. https://doi.org/10.1080/1064119X.2016.1275894.
Zhang, X., Zhang, C., Liu, Y. and Hu, Z. (2021), "Nondimensional parametric method for studying lateral cyclic response of offshore monopiles in sand", *Mar. Georesour. Geotec.*, **39**(4), 482-493. https://doi.org/10.1080/1064119X.2020.1717696.
Zhang, F., Okawa, K. and Kimura, M. (2008), "Centrifuge model test on dynamic behavior of group-pile foundation with inclined piles and its numerical simulation", *Front. Archit. Civ. Eng. China*, **2**(3), 233-241. https://doi.org/10.1007/s11709-008-0033-7.
Zheng, C., Liu, H., Ding, X. and Fu, Q. (2013), "Horizontal vibration of a large-diameter pipe pile in viscoelastic soil", *Math. Problem. Eng.*, **2013**(3), 1-13. 269493. https://doi.org/10.1155/2013/269493.
Zheng, C., Liu, H. and Ding, X. (2016), "Lateral dynamic response of a pipe pile in saturated soil layer", *Int. J. Numer. Anal. Method. Geomech*., **40**(2), 159-184. https://doi.org/10.1002/nag.2388.
Zhou, D., Lo, S.H., Au, F.T.K. and Cheung, Y.K. (2006), "Three-dimensional free vibration of thick circular plates on Pasternak foundation", *J. Sound Vib*., **292**(3-5), 726-741. https://doi.org/10.1016/j.jsv.2005.08.028.
Zhou, X.L. and Wang, J.H. (2009), "Analysis of pile groups in a poroelastic medium subjected to horizontal vibration", *Comput Geotech*, **36**(3), 406-418. https://doi.org/10.1016/j.compgeo.2008.08.013.
Zhu, B., Wu, X., Wang, Y. and Zhou, Y. (2021), "Centrifuge modelling for seismic response of single pile for wind turbine subjected to lateral load", *Mar. Georesour. Geotec.*, **39**(11), 1320-1338. https://doi.org/10.1080/1064119X.2020.1834654.

JS